DECLARATION OF GROUP AUTHORSHIP

This report has been prepared as a group project for the Chemical Laboratory Technology program at SAIT on April 24, 2025. The group members are Maisa Danaf and Gaby Yung.

We, Maisa Danaf and Gaby Yung, confirm that this work submitted for assessment is our own and is expressed in our own words. We both contributed to all parts of this report and the share of work is 50-50. All uses made within the Technology Report of the works of any other author, separate to the work group, in any form (ideas, equations, figures,texts, tables, programs), are properly acknowledged at the point of use. A list of the references used is included.

Maisa Danaf

Gaby Yung

BIOSORPTION OF SELENIUM IN CONTAMINATED WATER

Maisa Danaf, Gaby Yung

24/04/2025 SAIT CLT Capstone Project

Abstract

Selenium contamination in water, particularly from metallurgical coal mining, poses significant environmental and health risks. In Canada, the Elk River in Eastern British Columbia has been severely affected, with fish populations suffering due to elevated selenium levels. Current remediation costs are costly and produce secondary waste, underscoring the need for cost-effective and sustainable solutions. This project investigates the potential of orange peels, banana peels and corn cobs as biosorbents for selenium removal in contaminated water, leveraging their low cost and abundance as food waste. Employing batch adsorption tests, pH optimization, and pH drift experiments, selenium adsorption capacities and optimal conditions were systematically evaluated. Inductively Coupled Plasma-Optical Emission Spectroscopy (ICP-OES) analysis demonstrated modest adsorption efficiency, highlighting corn cob at a pH of 10 with an adsorption efficiency around 23.8%, albeit influenced by microbial activities that likely facilitated selenium reduction. The pH drift tests established points of zero charge (PZC), essential for optimizing conditions conducive to electrostatic adsorption. The project encountered methodological challenges, but despite lower-than-expected adsorption results, the findings helped establish parameters and testing methods for biosorption of selenium. Future studies should focus on improving testing methodologies, further characterization of biosorbents using Fourier-transform infrared spectroscopy (FTIR) and scanning electron microscopy (SEM), and explore microbial involvement in selenium biosorption. Ultimately, this study presents foundational knowledge toward environmentally sustainable biosorption solutions, promoting waste valorization and offering an affordable alternative to chemical remediation approaches.

Table of Contents

List of Figures

List of Tables

1. Introduction

Selenium contamination in water sources is a critical environmental and public health issue, particularly affecting regions with extensive surface mining activities, such as Elk Valley in Canada. Communities near these mining sites experience elevated selenium levels, leading to significant ecological disturbances and potential human health risks due to bioaccumulation and biomagnification (Elk River Alliance, 2025). This issue is gaining more traction in Alberta, with a proposed project for a metallurgical coal mine at Grassy Mountain currently seeking approval (Northback, 2024). The main concern is that potential selenium contamination could threaten major headwaters such as the Old Man River that act as major sources for ranching and agriculture. (*Grassy Mountain — Conserving Our Special Places*, n.d.) On the other hand, metallurgical coal is an essential component in the production of steel, which is necessary for all aspects of life around the globe (*Steel Production, Coking Coal - World Coal Association*, n.d.). The challenge we face is finding a balance between the necessity and economic implications of metallurgical coal, and the devastating environmental consequences of selenium pollution.

Conventional chemical remediation methods for selenium involve reagents that can be toxic, costly, and produce hazardous secondary wastes (Benis et al., 2021). As such, sustainable alternatives like biosorption have gained attention, employing agricultural waste and industrial byproducts as cost-effective and environmentally friendly biosorbents (Derco & Vrana, 2018; Jaishankar et al., 2014; Shamim, 2018). However, despite existing research, significant gaps remain regarding the biosorption efficiency of specific biomass types such as banana peels and corn cobs, as well as the absence of robust methodologies for testing selenium adsorption.

Therefore, this study aims to determine a suitable method to quantify adsorption of selenium using biosorbents and examine the optimal conditions for efficient selenium adsorption.

2. Literature Review

2.1 Properties of Selenium

Selenium (Se) is a metalloid exhibiting several oxidation states in aqueous solutions, predominantly selenite (Se(IV)), selenate (Se(VI)), elemental selenium (Se(0)), and selenide (Se^{2-}). The toxicity, mobility, and bioavailability of selenium are highly dependent on its chemical speciation, influenced by environmental parameters such as pH and oxidation-reduction potential (ORP) (Hasan & Ranjan, 2010). The Pourbaix diagram effectively illustrates the speciation behavior of selenium under varying conditions of pH and ORP.

Figures 1-3 indicate the major selenium species present in solution, with different solution matrixes and temperatures. Figure 1 indicates the speciation at 25°C, containing only aqueous species of selenium in water. Figure 2 shows the condition at 40°C, which approximates typical coal mine water temperatures, with all selenium species including elemental selenium. Figure 3 depicts a more complex scenario from an actual coal mine water matrix in China, demonstrating the influence of real environmental conditions such as the presence of mercury and magnesium giving rise to insoluble species (Shan et al., 2022). However, for the assessment of maximum adsorption efficiency under optimal parameters, this study utilized the simpler scenario of selenium in pure water at 25°C to maintain clarity and control over experimental variables.

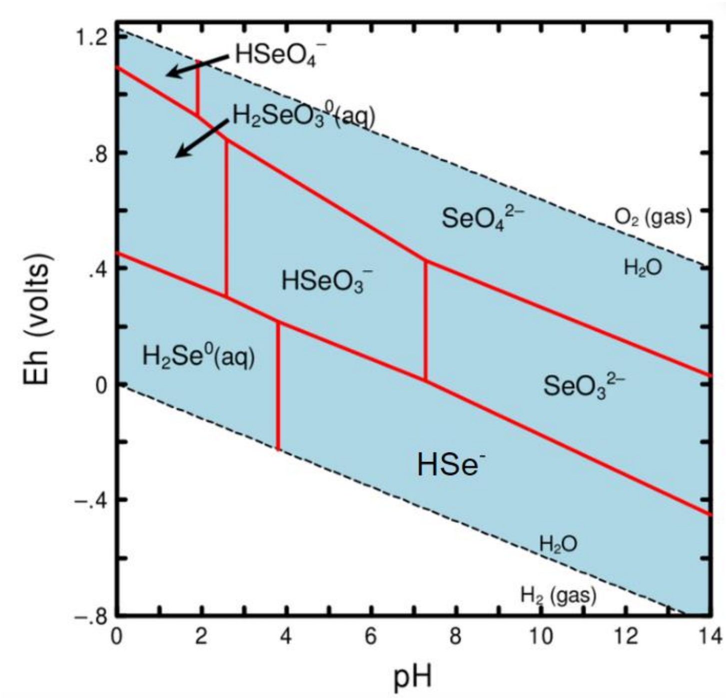

Figure 1: Speciation of selenium at 25°C in pure water with aqueous species only, adapted from Cantrell et al. (2007).

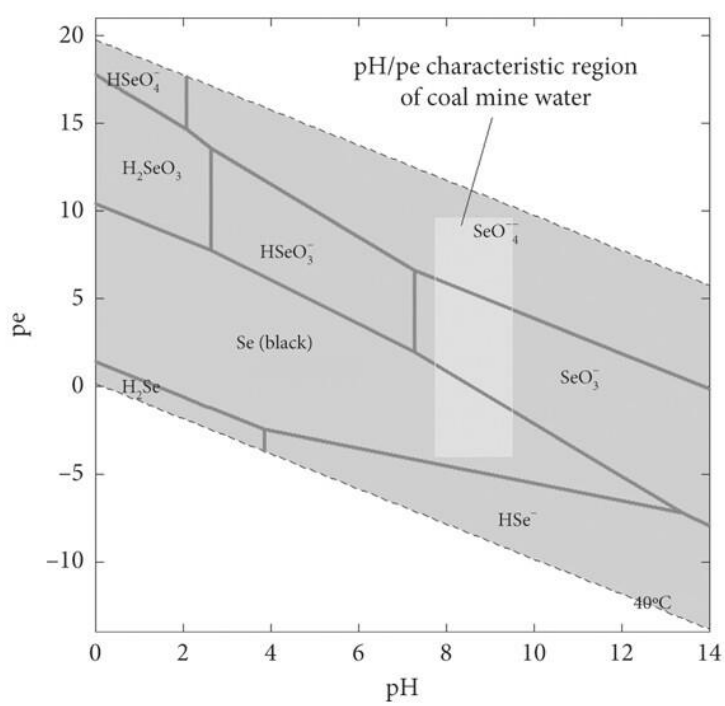

Figure 2: Speciation of selenium at 40°C in pure water with all species, from Shan et al. (2022).

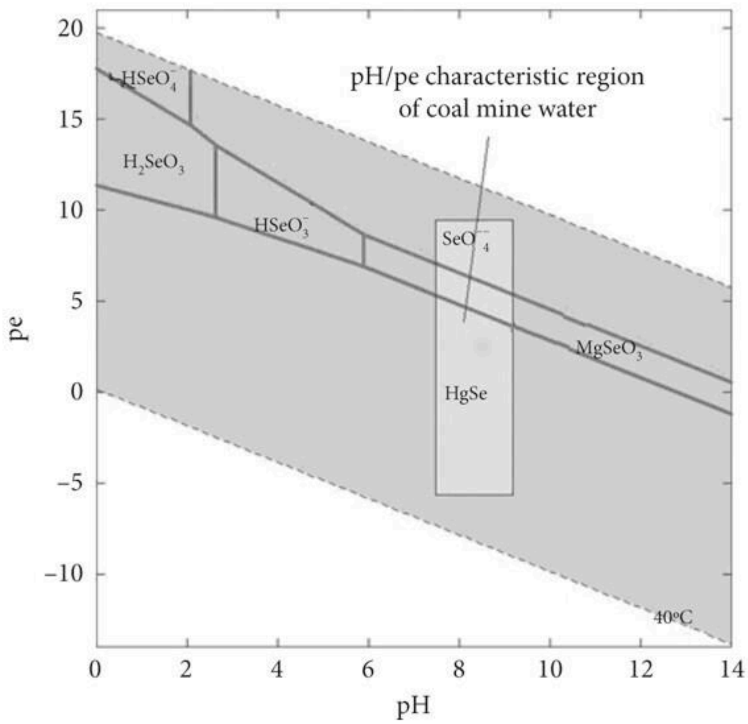

Figure 3: Speciation of selenium at 40°C in coal mine water from Xuzhou-Datun coal mine district in China, from Shan et al. (2022).

The environmental and health implications of selenium contamination are severe. Selenium toxicity can result in adverse ecological effects, including reproductive failure and deformities in aquatic life, and health problems in humans, such as gastrointestinal disturbances and neurological damage upon chronic exposure (Elk River Alliance, 2025). Hence, effective removal techniques are critical to safeguarding environmental health and preventing public health risks associated with selenium pollution. In this study, focus will be put on selenite removal as it has the highest biotoxicity (Hasan & Ranjan, 2010) and should be given more attention on removal methods.

2.2 Biosorption

Biosorption has emerged as a promising alternative to conventional chemical remediation methods for heavy metal removal, leveraging biological materials' natural adsorption capabilities (Abbas et al., 2014). Common biosorbents include living biomass such as bacteria, algae, fungi, as well as dead biomass derived from agricultural residues and industrial byproducts, presenting sustainable and economically viable solutions for pollutant removal (Shamim, 2018). Previous studies have demonstrated the efficacy of various agricultural waste materials in adsorbing heavy metals and contaminants from water, such as rice husks (Bansal et al., 2009), cabbage and cauliflower wastes (Hossain et al., 2013), peanut hull (Johnson et al., 2002) etc. Among the studies, orange peels banana peels and corn cobs stand out due to their availability, cost-effectiveness, and intrinsic adsorption characteristics (Berber-Villamar et al., 2018; Jaishankar et al., 2014).

Specifically, orange peels have shown promising adsorption capacities attributed to their rich composition of cellulose, hemicellulose, pectin, and lignin, which contain functional groups such as hydroxyl and carboxyl groups, capable of binding heavy metal ions effectively (Dev et al., 2020). Similarly, banana peels and corn cobs share comparable properties, containing various functional groups that can promote water pollutant adsorption (Akpomie & Conradie, 2020; Al-Ghouti et al., 2009). Yet their application in selenium removal has been relatively under-explored, highlighting a critical knowledge gap. There are many mechanisms that can be involved in biosorption, including complexation, chelation, ion exchange, and electrostatic interactions (Kanamarlapudi et al., 2018; Shamim, 2018). In this study, we hypothesise the mechanism involved is electrostatic interactions, as it is the most common mechanism identified in previous studies and the easiest to control factors involved.

However, despite substantial general research on biosorption, definitive methods for systematically assessing and comparing the selenium adsorption capacities of biosorbents remain inadequate. Current limitations include inconsistencies in experimental setups, conditions, and the absence of standardized testing methods, complicating comparative analyses and practical applications. (Liu & Liu, 2007) This proves the necessity of developing a standardized and robust method to effectively evaluate and optimize biosorbent performance specifically for selenium adsorption, thereby enhancing the practical viability of biosorption technologies in environmental remediation efforts.

3. Methodology

3.1 Material Preparation

The biosorbent materials were initially washed thoroughly with deionized (DI) water. After washing, they were air-dried and then placed in an oven at 60 °C until completely dry. The dried materials were subsequently crushed and ground using a blender, then passed through a 40-mesh sieve to ensure uniform particle size. For materials requiring activation, the sieved materials were treated with 0.1 N nitric acid while stirring at 120 rpm for 2–3 hours to saturate binding sites with hydrogen ions. Following activation, the materials were once again dried, crushed, and sieved using the same procedure. The prepared biosorbents were then stored in a desiccator until use. This procedure was adapted from our primary reference paper. (Dev et al., 2020)

3.2 pH Optimization

A volume of 25 mL of 50 ppm sodium selenite solution was pipetted into 4 sets of 12 beakers. The pH of the solutions was adjusted using HNO_3 and NaOH to achieve a pH range from 2 to 12 across the sets. A total of 0.05 g of each biosorbent type was weighed in duplicate for each pH value, totaling 12 samples. The biosorbents were added to the solutions across the pH range in duplicate (6 pH values × 2 replicates = 12 treatments). An additional set of pH-adjusted solutions (pH 2–12) was prepared without any biosorbent to serve as controls. All samples were allowed to react for 240 hours (10 days). After the contact period, the samples were filtered using a 0.45-micron syringe filter into glass test tubes for ICP analysis to determine the optimal pH for selenium adsorption. This procedure was adapted from our primary reference paper. (Dev et al., 2020)

3.3 pH Drift Test

The point of zero charge (PZC) is a critical parameter in determining the surface charge characteristics of adsorbents. The pH drift test is a straightforward yet effective method used to identify the PZC. This method involves adding the adsorbent to solutions of varying initial pH and measuring the final pH after equilibrium is reached. The PZC is identified at the point where no significant change in pH occurs. Below this pH, the adsorbent surface is positively charged, and above this pH, the surface becomes negatively charged. For selenium adsorption, particularly selenite ions (negatively charged), the adsorbent surface should ideally be positively charged to enhance attraction and adsorption efficiency.

To perform the pH drift test, beakers containing 100mL of 0.1N potassium nitrate weren adjusted to pH values of 2, 4, 6, 8, 10, and 12 using nitric acid and sodium hydroxide. Prepared biosorbents were added to each beaker and agitated at 150rpm for 48 hours to allow the systems to reach equilibrium. Following the 48-hour interaction, pH of each solution was measured again. The change in pH was then plotted to determine the PZC. This procedure was followed from (Berber-Villamar et al., 2018)

3.4 Batch Adsorption Test

Batch adsorption tests were conducted to determine adsorption efficiency over time, when the process will reach equilibrium, and to obtain data for potential kinetic modelling. Manipulated variables were concentration of selenium in solution and exposure time.

A volume of 100 mL of sodium selenite solution at concentrations of 2, 10, 20, 50, 80, and 100 ppm was pipetted in duplicate, resulting in 12 prepared samples for each material. The pH of each solution was adjusted as appropriate using sodium hydroxide or nitric acid. Solid samples were weighed in duplicate for each concentration, with masses ranging from 2 to 3 g. The initial pH and oxidation-reduction potential (ORP) of each solution were measured and recorded. The solid samples were then added to their respective solutions, which were stirred using a shaker set to 120 rpm, and the timer was started. At 30-minute intervals, aliquots were withdrawn from each solution, centrifuged to separate solids, and the supernatants were filtered using a syringe and 0.45-micron filter into glass test tubes for subsequent ICP analysis. This sampling process was repeated at 30-minute intervals for a total duration of 150 minutes (five time points). Following the final sampling, the pH and ORP of each solution were again measured and recorded. The pH and ORP values were used to estimate the main species of selenium in solution before and after treatment. This procedure was adapted from our primary reference paper. (Dev et al., 2020)

3.5 ICP

Adsorption of selenium was quantified via Inductively Coupled Plasma-Optical Emission Spectroscopy (ICP-OES). Solutions were analyzed after each batch test to determine the concentration of selenium remaining in solution and adsorption efficiency of each parameter. The concentrations of standards and quality control (QC) samples are detailed in Table 1 below. To maintain confidence in the results of the analysis, QC duplicates were measured every after every 12 samples, and a recalibration was performed after every 24 samples. The chosen wavelength for analysis was 196.026nm.

Table 1: Concentrations of Na_2SeO_3 in Standard and QC Solutions for ICP Analysis

	Standard 1	**Standard 2**	**Standard 3**	**Standard 4**	**Standard 5**	**Low QC**	**High QC**
Concentration Na_2SeO_3 (mg/L)	1.00	20.00	50.00	100.00	120.00	10.00	80.00

4. Data

4.1 pH Optimization

Table 2 summarizes the data from the pH optimization test. Detailed results obtained from ICP analysis can be found in appendix A.1.

Table 2: pH Optimization Data

Biosorbent	pH	Initial Concentration (mg/L Se)	Final Concentration (mg/L Se)	Adsorption Efficiency (% Adsorbed)
Orange Peel	2	48.077	42.745	11.090
	4	49.920	47.86	4.127
	6	48.544	47.03	3.118
	8	49.407	47.825	3.202
	10	49.900	48.655	2.495
	12	48.077	44.995	6.410
Banana Peel	2	48.077	46.66	2.9472
	4	49.920	48.30	3.24544
	6	48.544	46.15	4.931
	8	49.407	47.62	3.61712
	10	49.900	48.5	2.806
	12	48.077	47.705	0.7736
Corn Cob	2	48.077	46.59	3.0928
	4	49.920	49.255	1.332384
	6	48.544	47.5	2.15
	8	49.407	48.28	2.28128
	10	49.900	38.015	23.81794
	12	48.077	47.64	0.9088

Control	2	48.077	44.795	6.8264
	4	49.920	49.965	0
	6	48.544	48.915	0
	8	49.407	50.28	0
	10	49.900	51.345	0
	12	48.077	45.155	6.0776

4.2 pH Drift Test

Table 3: pH Drift Test Data

Biosorbent	Initial pH	Final pH	Δ pH
Orange Peel	2.07	2.39	-0.32
	4.07	4.08	-0.01
	6	3.93	2.07
	8.07	4.09	3.98
	9.93	4.12	5.81
	11.95	4.77	7.18
Banana Peel	2.04	2.26	-0.22
	4.01	5.57	-1.56
	6	5.94	0.06
	7.97	6.21	1.76
	10.07	5.69	4.38
	11.99	10.88	1.11
Corn Cob	2.04	2.09	-0.05
	4.01	3.86	0.15
	6	6.39	-0.39
	7.97	5.65	2.32
	10.07	7.53	2.54
	11.99	11.52	0.47

4.3 Batch Adsorption Test

Tables 4 and 5 summarize the data collected from batch adsorption test. Detailed results obtained from ICP analysis can be found in appendix A.2.

Table 4: Batch Adsorption Test Data

Exposure Time (minutes)	Initial Concentration (mg/L Se)	Final Concentration (mg/L Se)	Adsorption Efficiency (% Adsorbed)
30	2	1.95	2.5
	2	1.88	6
	10	10.19	0
	10	9.83	1.7
	20	19.41	2.95
	20	19.61	1.95
	50	50.8	0
	50	49.44	1.12
	80	79.4	0.75
	80	79.99	0.0125
	100	98.76	1.24
	100	100.33	0
60	2	1.93	3.5
	2	1.86	7
	10	9.69	3.1
	10	9.81	1.9
	20	20.1	0
	20	20.02	0
	50	51.29	0
	50	50.75	0
	80	81.56	0
	80	81.75	0
	100	102.72	0
	100	99.96	0.04
90	2	1.89	5.5
	2	1.95	2.5
	10	9.95	0.5
	10	10.14	0

	20	20.73	0
	20	20.51	0
	50	50.22	0
	50	52.15	0
	80	79.57	0.5375
	80	83.28	0
	100	103.47	0
	100	98.93	1.07
120	2	1.96	2
	2	1.81	9.5
	10	9.97	0.3
	10	9.7	3
	20	20.49	0
	20	20.49	0
	50	51.7	0
	50	51.18	0
	80	80.61	0
	80	84.27	0
	100	101.89	0
	100	102.81	0
150	2	1.83	8.5
	2	1.76	12
	10	9.82	1.8
	10	9.7	3
	20	19.73	1.35
	20	19.57	2.15
	50	51.21	0
	50	51.01	0
	80	80.32	0
	80	83.26	0
	100	99.64	0.36
	100	101.25	0

Table 5: pH and ORP Data from Corn Cob Batch Adsorption Test

Concentration Na_2SeO_3 (mg/L)	Mass of Corn Cob (g)	Initial ORP (mV)	Final ORP (mV)	Δ ORP (mV)	Initial pH	Final pH	Δ pH
2.00	2.0003	67.7	260.5	192.8	7.77	3.12	-4.65
2.00 Duplicate	1.999	79.5	265.9	186.4	7.53	3.13	-4.40
10.00	1.9979	106.2	260.9	154.7	7.27	3.17	-4.10
10.00 Duplicate	1.9639	104.9	271.1	166.2	7.31	3.17	-4.14
20.00	1.9766	119.7	274.6	154.9	7.64	3.24	-4.40
20.00 Duplicate	1.9679	119.4	273.0	153.6	7.88	3.24	-4.64
50.00	1.9868	106.8	172.5	65.7	7.89	3.98	-3.91
50.00 Duplicate	1.9884	95.7	183.5	87.8	8.35	3.94	-4.41
80.00	1.9621	102.9	205.7	102.8	8.1	3.65	-4.45
80.00 Duplicate	1.9742	97.9	186.9	89	8.33	4.28	-4.05
100.00	1.9727	103.4	209.4	106	8.11	3.8	-4.31
100.00 Duplicate	1.9478	94.3	211.5	117.2	8.55	3.76	-4.79

5. Calculations

Below are the calculations used for analysis, only sample calculations are shown.

Adsorption Efficiency (% Adsorbed)

$$\%\,Adsorbed = \frac{c_i - c_f}{c_i} \times 100\%$$

$$\%\,Adsorbed = \frac{48.077\,mg/L\,Se - 42.745\ mg/L\,Se}{48.077\,mg/L\,Se} \times 100\%$$

$$\%\,Adsorbed = 11.090\%$$

Change in pH (Δ pH)

$$\Delta\,pH = \ pH_i - pH_f$$

$$\Delta\,pH = \ 2.07 - 2.39$$

$$\Delta\,pH = \ -0.32$$

Change in ORP (Δ ORP)

$$\Delta\,ORP = \ ORP_i - ORP_f$$

$$\Delta\,ORP = \ 67.7mV - 260.5mV$$

$$\Delta\,ORP = \ 192.8mV$$

Precision (% Relative Difference)

$$\%RD = \frac{A - B}{A + B} \times 200\%$$

$$\%RD = \frac{98.2\, mg/L\, Se - 10.03\, mg/L\, Se}{98.2\, mg/L\, Se + 10.03\, mg/L\, Se} \times 200\%$$

$$\%RD = -2.116\%$$

Accuracy (% Readback)

$$\%RB = \frac{measured}{true} \times 100\%$$

$$\%RB = \frac{9.82\, mg/L\, Se}{10.00\, mg/L\, Se} \times 100\%$$

$$\%RB = 98.2\%$$

6. Graphs

6.1 pH Optimization

Figure 4 shows the percentage of selenium adsorption after pH optimization test.

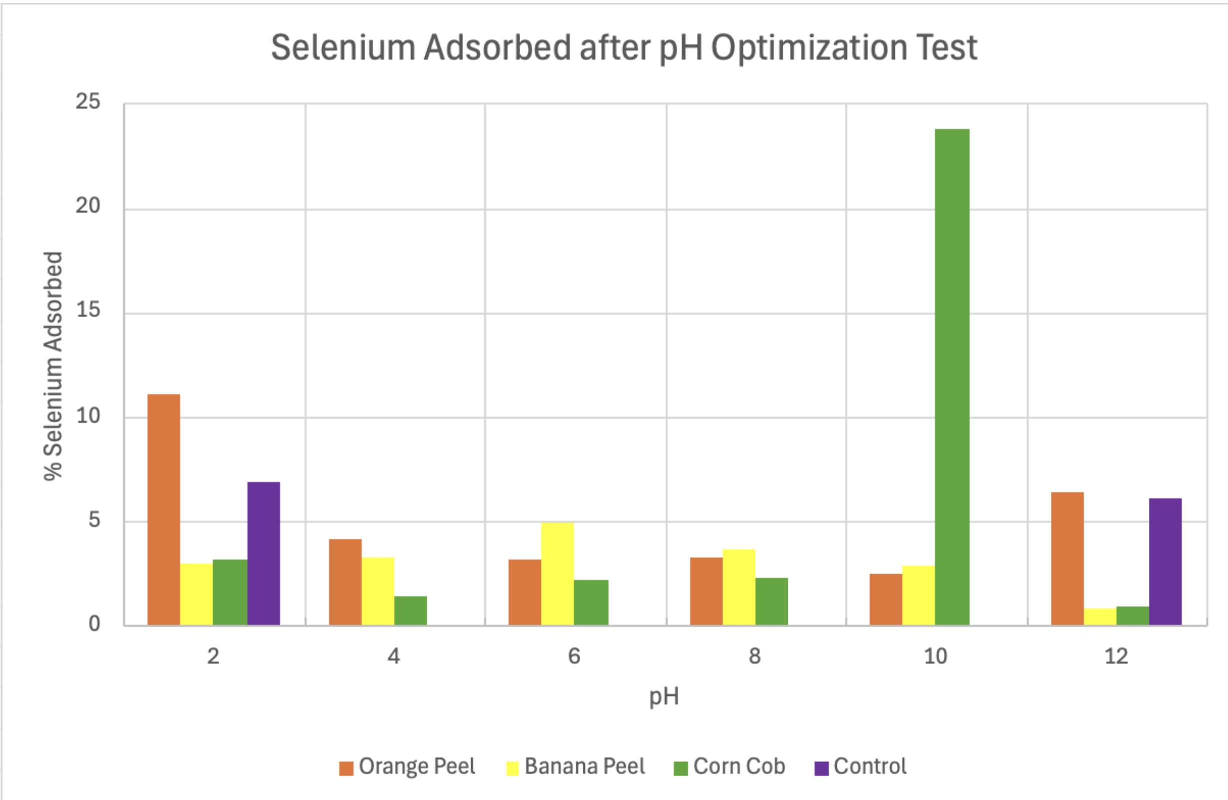

Figure 4: Selenium Adsorbed after pH Optimization Test

6.2 pH Drift Test

Results for pH drift test and indicated point of zero charge is indicated in Figure 5.

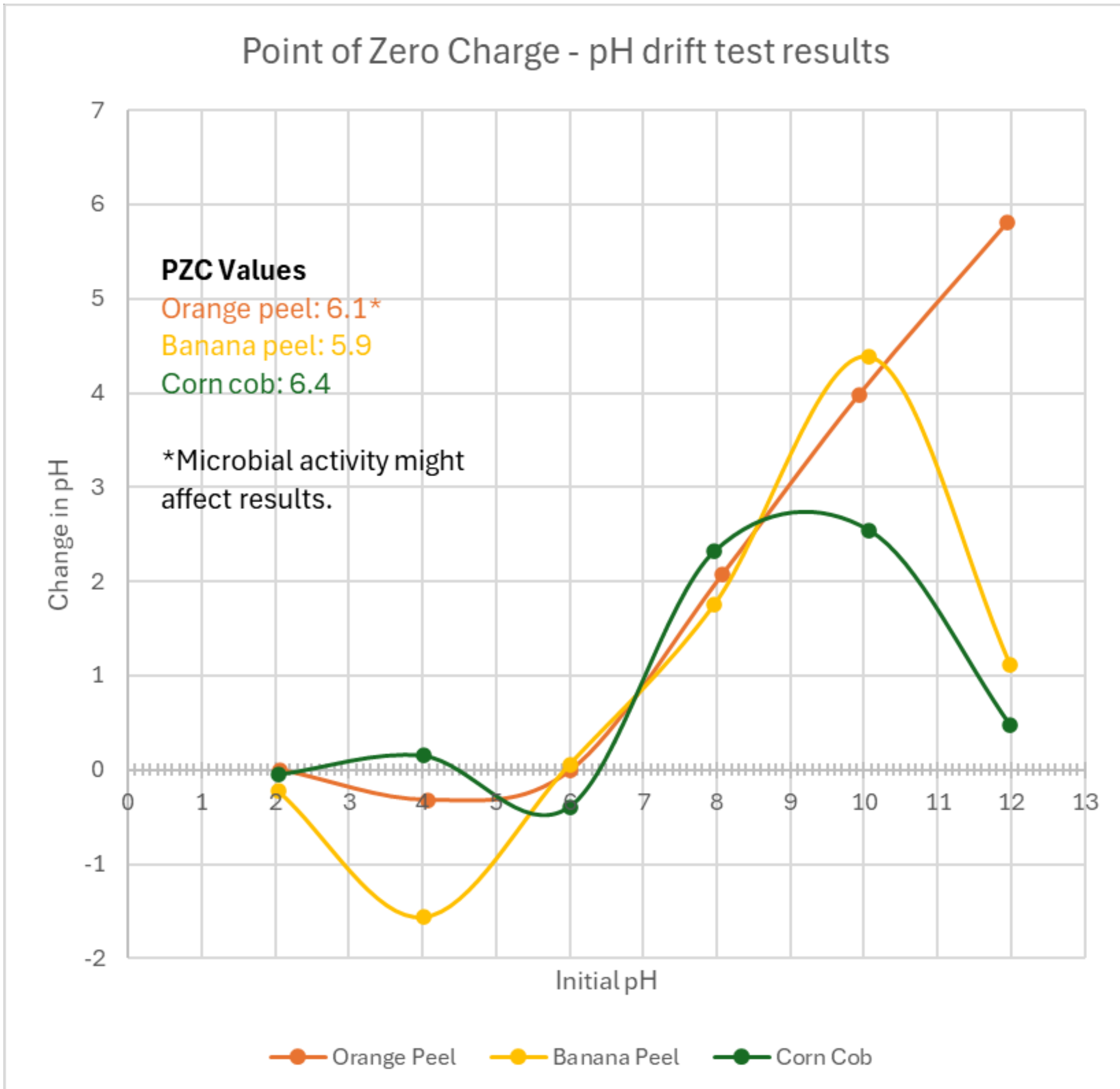

Figure 5:Point of Zero Charge - pH Drift Test Results

6.3 Batch Adsorption Test

Figure 6 shows the percentage of selenium adsorption for batch adsorption test by corn cob. ORP and pH measured before and after the test is plotted on a Pourbaix diagram in Figure 7.

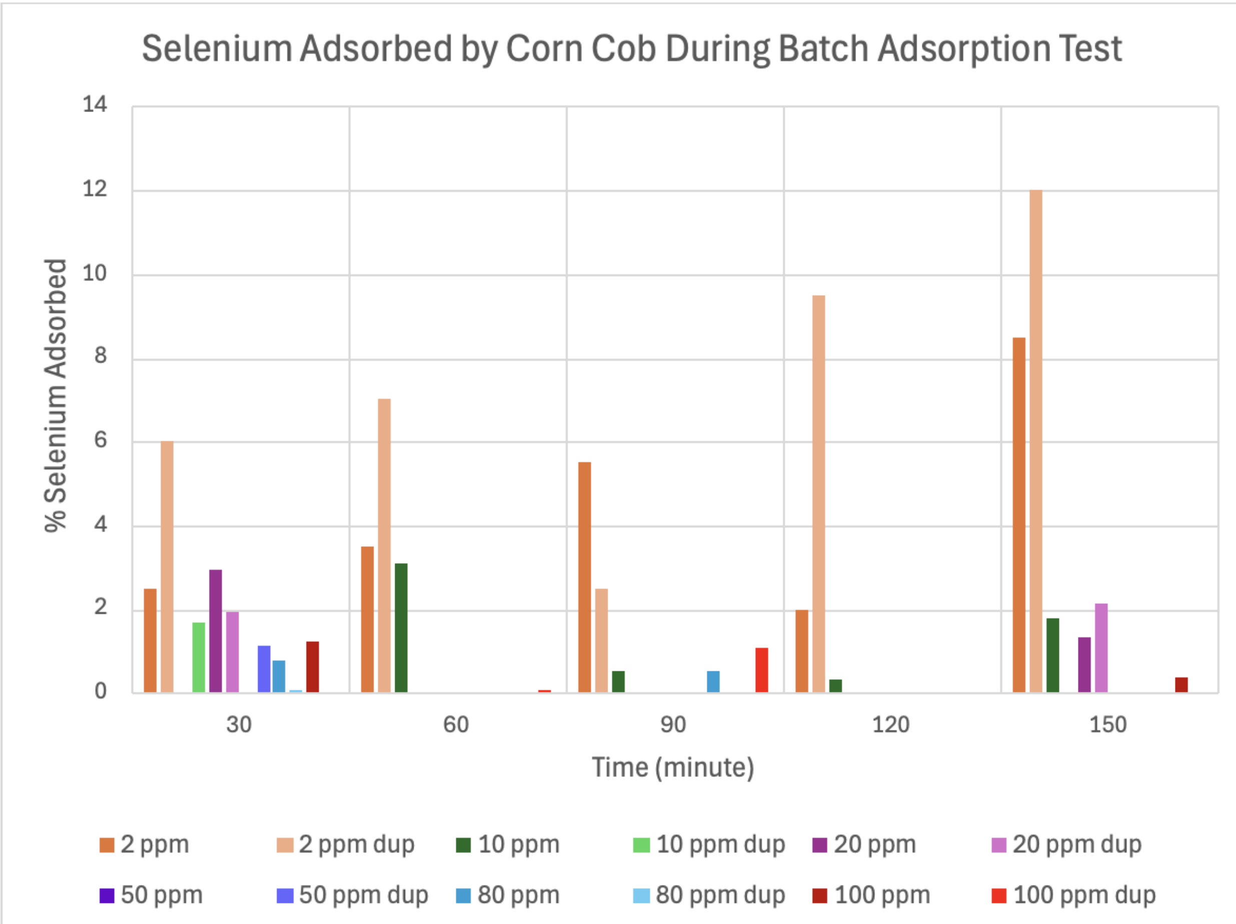

Figure 6: Selenium Adsorbed by Corn Cob During Batch Adsorption Test

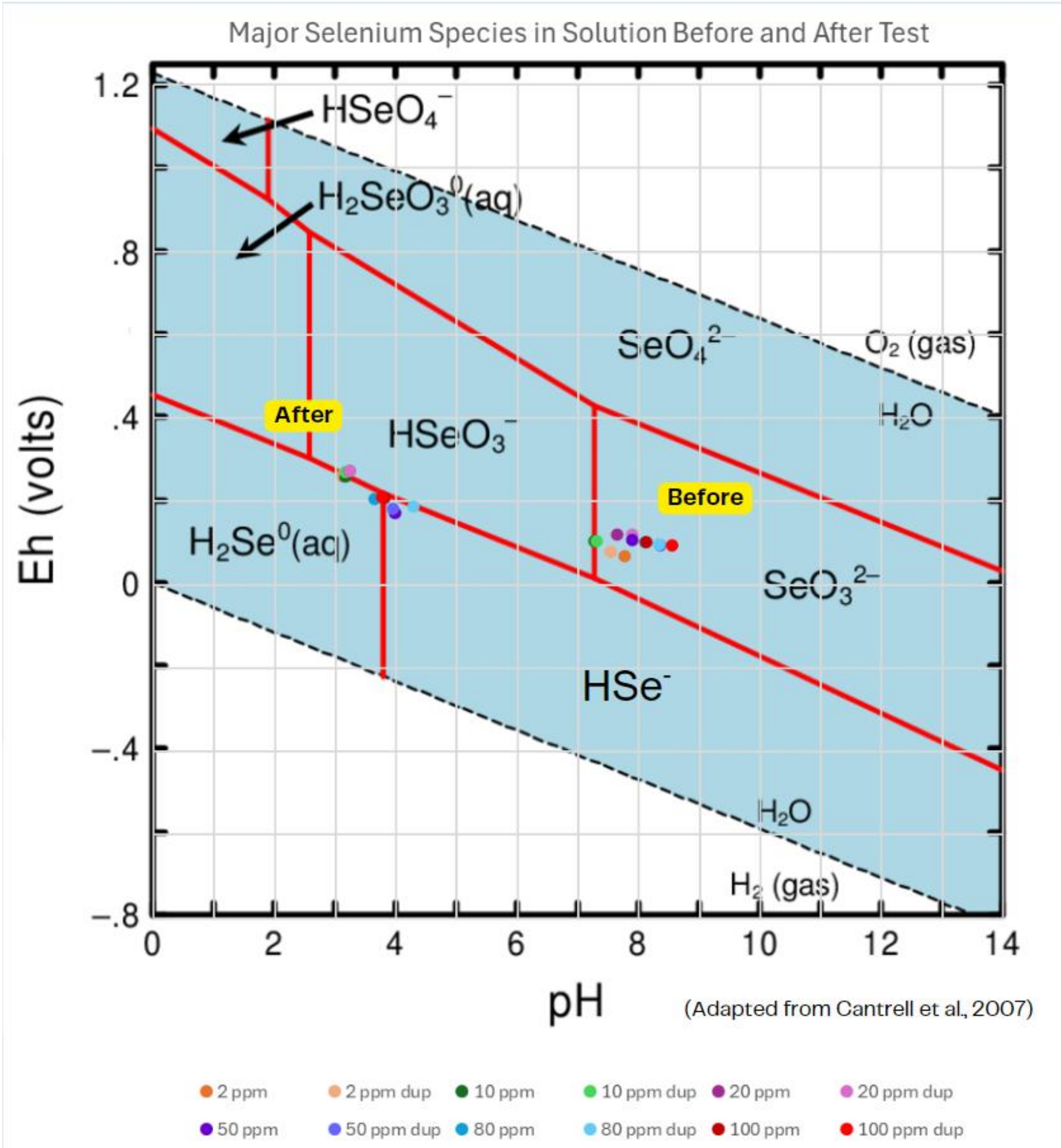

Figure 7: pH and ORP of solutions before and after adsorption test.

7. Results

7.1 pH Optimization

Table 6 summarizes the quality control results for pH optimization test on ICP.

Table 6: Quality Control Data from pH Optimization Test

Sample ID	Measured Concentration (mg/L)	Precision (%RD)	Acceptability (±20%)	Accuracy (%RB)	Acceptability (±10%)
Low QC 1	9.82	-2.116	Pass	98.2	Pass
Low QC 2	10.03	0.8008	Pass	100.3	Pass
Low QC 3	9.95	0.4028	Pass	99.5	Pass
Low QC 4	9.91	-0.5033	Pass	99.1	Pass
Low QC 5	9.96	0.5033	Pass	99.6	Pass
High QC 1	77.82	-5.097	Pass	97.28	Pass
High QC 2	81.89	1.861	Pass	102.4	Pass
High QC 3	80.38	-0.5706	Pass	100.5	Pass
High QC 4	80.84	-0.6043	Pass	101.1	Pass
High QC 5	81.33	0.6043	Pass	101.7	Pass

7.2 pH Drift Test

Table 7 shows the PZC for the biosorbents as obtained from the pH drift test.

Table 7: Point of Zero Charge Results from pH Drift Test

Biosorbent	Orange Peel	Banana Peel	Corn Cob
Point of Zero Charge (PZC)	6.1*	5.9	6.4

*Microbial activity during testing might affect results.

7.3 Batch Adsorption Test

Table 8 summarizes the quality control results for pH optimization test on ICP.

Table 8: Quality Control Results from Batch Adsorption Test

Sample ID	Measured Concentration (mg/L)	Precision (%RD)	Acceptability (±20%)	Accuracy (%RB)	Acceptability (±10%)
Low QC 1	10.03	2.729	Pass	100.3	Pass
Low QC 2	9.76	-1.525	Pass	97.6	Pass
Low QC 3	9.91	1.525	Pass	99.1	Pass
Low QC 4	9.76	-2.129	Pass	97.6	Pass
Low QC 5	9.97	2.129	Pass	99.7	Pass
High QC 1	80.77	2.685	Pass	101.0	Pass
High QC 2	78.63	-1.940	Pass	98.29	Pass
High QC 3	80.17	1.142	Pass	100.2	Pass
High QC 4	79.26	-1.104	Pass	99.08	Pass
High QC 5	80.14	1.104	Pass	100.2	Pass

8. Discussion

8.1 Analysis of Results

8.1.1 pH Optimization

There was no significant adsorption of selenium observed after the pH optimization test. The highest result observed was 23.8% adsorption in the solution containing corn cob at a pH of 10, though the sample and solution were obviously discoloured to a bright orange colour as shown in Figure 8. Further investigation indicated that the change in selenite concentration was likely due to elemental selenium deposition or bacterial influence.

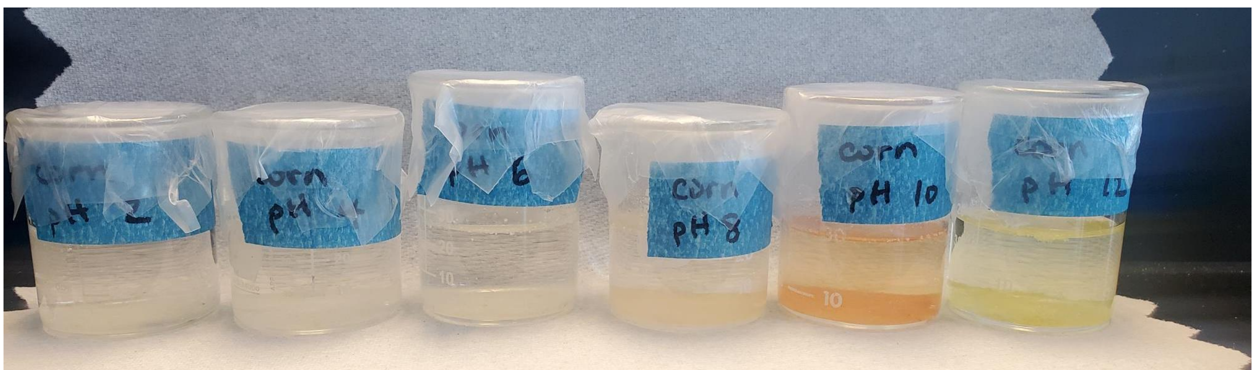

Figure 8: Solutions Containing Corn Cob after pH Optimization Test

There have been studies about bacteria isolated from a river in South Korea, which has shown ability to reduce selenite to elemental selenium nanoparticles in basic conditions up to pH 10 (Won et al., 2021). We suspect that a similar event happened for the corn pH 10 test results, as it showed the same signature bright orange color of selenium nanoparticles, has a sticky texture that resembles bacterial colony, and can be completely filtered away, leaving a clear solution. The bacteria strain might originate from the water source, in the air, or with the corn cob, and the corn cob could have provided a good medium for the bacteria to grow.

8.1.2 pH Drift Test

The PZC results not only provided information about the pH needed for the surface to have a positive charge, but also indicated specific optimal pH ranges where surfaces can maintain a positive charge without structural damage from extreme pH environments. Orange peel testing exhibited potential inaccuracies due to signs of microbial contamination during the test, suggesting that results for this biosorbent might require further validation. Previous studies indicated that the PZC for orange peel should be at around 3.85, (Afolabi et al., 2022) and should be a good indicator for reference.

8.1.3 Batch Adsorption Test

The batch adsorption tests yielded lower-than-anticipated results, showing approximately 8-10% adsorption at a selenium concentration of 2 ppm after 2.5 hours, with negligible adsorption observed at other tested concentrations. Figure 7 plotted the measurement of ORP and pH before and after treatment onto the Pourbaix diagram for selenium in water at 25°C, which helps predict the speciation of selenium throughout the test. There is an overall lowering of pH, indicating that the hydrogen ions added onto the surface of biosorbent during the activation process are likely diffused into the solution. Additionally, the biosorbents introduced a slightly reducing environment, which lowers the ORP relative to pH, shifting selenium species towards less charged or uncharged forms, thus leading to reduced selenium adsorption or potential desorption.

8.2 Challenges

Several challenges were encountered during the course of this study. Firstly, sample preparation proved challenging, particularly grinding biosorbents to the desired particle size. Multiple methods were attempted before identifying coffee grinders as an effective yet inefficient solution. This method proved slow, restricted to small batches, and susceptible to overheating. Additionally, test design posed difficulties. While numerous methods exist for measuring heavy metal biosorption efficiency, they do not adequately apply to selenium, a metalloid. Furthermore, the biosorption mechanism for selenium remains largely unknown, requiring significant guesswork and trial-and-error experimentation. We also encountered practical issues with replicating previously reported methods, as many studies lacked sufficient detail or required unavailable equipment or apparatus. Finally, time constraints are another big factor, as full adsorption tests typically require five hours, we had to shorten the test time to 2.5 hours to fit within allocated lab times, including setup and cleanup.

8.3 Key Findings

8.3.1 pH and ORP

Our findings confirmed that selenium adsorption and desorption are strongly influenced by pH and ORP, which affect selenium speciation. These variables must be carefully controlled to prevent a reaction shift to desorption due to changing conditions or other contributing reactions. Desorption after treatment would release selenium back into water, which could have catastrophic consequences. Adsorption relies on negatively charged selenium species and a positively charged sorbent surface to facilitate electrostatic attraction. In some cases, sorbents were activated by pre-treating with nitric acid to the saturate binding sites with hydrogen ions. The point of zero charge PZC was instrumental in understanding and predicting these interactions, as it indicates the pH at which the sorbent surface carries no net charge. Operating below the PZC ensured a positively charged surface, enhancing selenium uptake.

8.3.2 Matrix Interferences

While biosorption presents a promising and sustainable approach for selenium removal, the use of organic materials introduces certain complexities. Biological or organic additions to the treatment matrix can lead to unpredictable interferences and competing reactions that are difficult to control. This is particularly relevant in systems where the sorbent material is itself organic, as was the case in this study.

The organic nature of the biosorbents creates an ideal environment for microbiological growth. Over time, microbial activity can alter the chemical conditions of the system, potentially affecting selenium speciation and the stability of adsorbed species. In some cases, microbial processes may produce byproducts or biofilms that interfere with selenium binding, leading to inconsistent or misrepresented results. (Shamim, 2018)

8.3.3 Other Contributing Mechanisms

Although electrostatic attraction was identified as the primary mechanism for selenium adsorption in our experiment, it is likely that additional mechanisms also contributed—many of which were beyond the scope of our experimental design to isolate or quantify, with gaps in existing research adding further limitations. The complexity of biosorption, especially when using organic materials, makes it difficult to account for all interactions involved.

Functional groups, such as hydroxyl, carboxyl, or amine groups, can play a significant role in binding selenium and other heavy metals. (Dev et al., 2020) For example, previous research has shown that hydroxyl groups on orange peels are responsible for selenium bonding, suggesting similar mechanisms may be at play with the other materials we used. (Mora et al., 2020) This mechanism can be qualified using FTIR, which we were unable to investigate in this study due to time constraints.

8.4 Future Recommendations

Several future recommendations are proposed as selenium biosorbent testing methods to be used in future studies. Initially, pH drift test should be conducted to identify biosorbents with higher PZC, ideally in neutral or basic ranges, to enhance electrostatic interactions with negatively charged selenium species. It is recommended to avoid artificial pH adjustments during experiments, allowing for a more accurate representation of natural speciation and biosorption processes. Determining the adsorption effect timeline is crucial, hence clearly defining whether short-term (~3-5 hours) or long-term (~days) interactions are being evaluated will significantly influence experimental designs.

Monitoring solution ORP and pH before, during, and after adsorption tests is vital, as these parameters aid in predicting selenium speciation, which will affect adsorption efficiency and reliability of results. The use of a shaker combined with strainers or centrifugation methods could streamline the quenching and solution recovery process during adsorption tests. To help understanding adsorption mechanisms, we suggest the use of other analytical techniques like Fourier-transform infrared spectroscopy (FTIR) for identifying functional groups involved, and scanning electron microscopy (SEM) for visualizing surface characteristics and confirming selenium adsorption.

Moreover, bacterial removal might utilize a slower metabolism pathway to form complexes with elemental selenium opens up new possibilities, which could provide insights into additional bioremediation methods. Finally, encapsulating biosorbents in alginate gel is suggested to prevent alterations in matrix conditions such as pH and ORP. This encapsulation could maintain the stability of the adsorption environment, ensuring the effectiveness of the charge-to-charge attraction mechanism, while also simplifying biosorbent handling and retrieval during practical applications.

9. Conclusion

In this study, we have conducted pH optimization test and batch adsorption test of selenium using orange peels, banana peels, and corn cob, and quantified the percentage adsorbed using ICP-OES. We also used pH drift test to determine point of zero charge for the biosorbents, determined a suitable method for biosorbent selenium adsorption efficiency testing and suggested some optimal parameters. Further research directions are recommended, and we believe that biosorbents have the potential to support a future of responsible coal mining and sustainable selenium treatment in water.

10. Acknowledgements

We would like to express our gratitude to all the people who have helped throughout this project, especially our instructors in charge of the capstone project course: Chris Sadak, Raphael Dong, Melani Sooriyaarachchi, and Thilina Jayawardana for their guidance along the way, Andrew Jones for spending the time to discuss with us about the theory aspects of this project, Camille Scheibner for suggesting methods to process the biosorbents, and our laboratory technologists: Krysta Abernathy, Ryan Walters, and Arnel Angeles for supplying chemicals and equipment and always providing support in the lab.

11. References

Abbas, H., Sulaymon, Salman H. Abbas, Ibrahim M. Ismail, Tarek M. Mostafa, & Abbas H. Sulaymon. (2014). Biosorption of Heavy Metals: a review. In *Journal of Chemical Science and Technology* (pp. 74–102).

Afolabi, F. O., Musonge, P., & Bakare, B. F. (2022). Adsorption of Copper and Lead Ions in a Binary System onto Orange Peels: Optimization, Equilibrium, and Kinetic Study. *Sustainability*, *14*(17), 10860. https://doi.org/10.3390/su141710860

Akpomie, K. G., & Conradie, J. (2020). Banana peel as a biosorbent for the decontamination of water pollutants. A review. *Environmental Chemistry Letters*, *18*(4), 1085–1112. https://doi.org/10.1007/s10311-020-00995-x

Al-Ghouti, M. A., Li, J., Salamh, Y., Al-Laqtah, N., Walker, G., & Ahmad, M. N. (2009). Adsorption mechanisms of removing heavy metals and dyes from aqueous solution using date pits solid adsorbent. *Journal of Hazardous Materials*, *176*(1–3), 510–520. https://doi.org/10.1016/j.jhazmat.2009.11.059

Bansal, M., Singh, D., Garg, V. K., & Rose, P. (2009). Use of agricultural waste for the removal of nickel ions from aqueous solutions: Equilibrium and kinetics studies. In *International Journal of Civil, Environmental, Structural, Construction and Architectural Engineering* (Vols. 3–3, pp. 174–174). https://scholar.waset.org/1999.3/10484

Benis, K. Z., McPhedran, K. N., & Soltan, J. (2021). Selenium removal from water using adsorbents: A critical review. *Journal of Hazardous Materials*, *424*, 127603. https://doi.org/10.1016/j.jhazmat.2021.127603

Berber-Villamar, N. K., Netzahuatl-Muñoz, A. R., Morales-Barrera, L., Chávez-Camarillo, G. M., Flores-Ortiz, C. M., & Cristiani-Urbina, E. (2018). Corncob as an effective, ecofriendly, and economic biosorbent for removing the azo dye Direct Yellow 27 from aqueous solutions. *PLoS ONE*, *13*(4), e0196428. https://doi.org/10.1371/journal.pone.0196428

Cantrell, K. J., Zachara, J. M., Dresel, P. E., Krupka, K. M., & Serne, R. J. (2007). *Geochemical Processes data package for the VADOSE zone in the Single-Shell Tank waste management areas at the Hanford site*. https://doi.org/10.2172/917584

Derco, J., & Vrana, B. (2018). Introductory chapter: Biosorption. In *InTech eBooks*. https://doi.org/10.5772/intechopen.78961

Dev, S., Khamkhash, A., Ghosh, T., & Aggarwal, S. (2020). Adsorptive removal of SE(IV) by citrus peels: Effect of adsorbent entrapment in calcium alginate beads. *ACS Omega*, *5*(28), 17215–17222. https://doi.org/10.1021/acsomega.0c01347

Grassy mountain — conserving our special places. (n.d.). Conserving Our Special Places. https://www.livingstonelandowners.net/grassy-mountain#:~:text=Project%20Overview,wildlife%20and%20sensitive%20water%20systems.

Hasan, S. H., & Ranjan, D. (2010). Agro-Industrial waste: a Low-Cost option for the biosorptive remediation of selenium anions. *Industrial & Engineering Chemistry Research*, *49*(19), 8927–8934. https://doi.org/10.1021/ie100622c

Hossain, M., Ngo, H., Guo, W., Nguyen, T., & Vigneswaran, S. (2013). Performance of cabbage and cauliflower wastes for heavy metals removal. *Desalination and Water Treatment*, *52*(4–6), 844–860. https://doi.org/10.1080/19443994.2013.826322

Jaishankar, M., Mathew, B. B., Shah, M. S., Murthy, T. P. K., & Gowda, K. R. S. (2014). Biosorption of few heavy metal ions using agricultural wastes. *Journal of Environment Pollution and Human Health*, *2*(1), 1–6. https://doi.org/10.12691/jephh-2-1-1

Johnson, P., Watson, M., Brown, J., & Jefcoat, I. (2002). Peanut hull pellets as a single use sorbent for the capture of Cu(II) from wastewater. *Waste Management*, *22*(5), 471–480. https://doi.org/10.1016/s0956-053x(01)00036-8

Kanamarlapudi, S. L. R. K., Chintalpudi, V. K., & Muddada, S. (2018). Application of Biosorption for Removal of Heavy Metals from Wastewater. In *InTech eBooks*. https://doi.org/10.5772/intechopen.77315

Liu, Y., & Liu, Y. (2007). Biosorption isotherms, kinetics and thermodynamics. *Separation and Purification Technology*, *61*(3), 229–242. https://doi.org/10.1016/j.seppur.2007.10.002

Mora, B. P., Bertoni, F. A., Mangiameli, M. F., González, J. C., & Bellú, S. E. (2020). Batch and fixed-bed column studies of selenite removal from contaminated water by orange peel-based sorbent. *Water Science and Engineering*, *13*(4), 307–316. https://doi.org/10.1016/j.wse.2020.12.003

Northback. (2024, December 17). *Northback*. https://northback.ca/?https%3A%2F%2Fnorthback_ca%2F%3Futm_medium=ad&utm_source=google&gad_source=1&gbraid=0AAAAA-T9wGa6PhK34XLA4KsS_XjPCSFzw&gclid=CjwKCAjwwqfABhBcEiwAZJjC3rKIO02C4twG2Zpr9jfJ70fLD35SEHFazoXdHjKNM0WonYZJhqwDahoCbHgQAvD_BwE

Shamim, S. (2018). Biosorption of heavy metals. In *InTech eBooks*. https://doi.org/10.5772/intechopen.72099

Shan, Y., Qin, Y., & Wang, W. (2022). Selenium Migration Mode in Coal Seams: Insights from Multivariate Analysis, Leaching Investigation, and Modelling. *International Journal of Chemical Engineering*, *2022*, 1–14. https://doi.org/10.1155/2022/6189492

steel production, coking coal - World Coal Association. (n.d.). https://www.energybc.ca/cache/coal/www.worldcoal.org/coal/uses-of-coal/coal-steel/index.html

Won, S., Ha, M., Nguyen, D. D., & Kang, H. Y. (2021). Biological selenite removal and recovery of selenium nanoparticles by haloalkaliphilic bacteria isolated from the Nakdong River. *Environmental Pollution*, *280*, 117001. https://doi.org/10.1016/j.envpol.2021.1

12. Appendix

A. ICP Data

A.1 pH Optimization ICP Data

Test Report

Agilent Technologies

Summary

Worksheet Name	GM Capstone pH Data.esws	Created Date/Time (local)	2025-02-27 2:26:46 PM
Instrument Name	MY2240CQ23	Created Date/Time (GMT)	2025-02-27 9:26:46 PM
Software Version	7.6.0.12121	Workstation Name	DESKTOP-7NFNNVR
Firmware Version	5590	Report Generated By	DESKTOP-7NFNNVR\ICP-OES

File Path D:\ICP-OES\Documents\Students\Worksheets\GM Capstone pH Data.esws

Notes

Elements

Element	Wavelength (nm)	Label	Type	Internal Standard	Background Correction	Calibration Fit	Condition Set
Se	196.026	Se (196.026 nm)	Analyte		Fitted	Linear Weighted	1
Se	203.985	Se (203.985 nm)	Analyte		Fitted	Linear Weighted	1

Sequence

Rack:Tube	Sample Label	Weight (g)	Volume (mL)	Dilution
S1:1	Blank	1	1	1
S1:2	Standard 1	1	1	1
S1:3	Standard 2	1	1	1
S1:4	Standard 3	1	1	1
S1:5	Standard 4	1	1	1
S1:6	Standard 5	1	1	1
S1:11	Low QC Dup	1	1	1
S1:12	High QC Dup	1	1	1
1:1	ORANGE 2	1	1	1
1:2	ORANGE 2 DUP	1	1	1
1:3	ORANGE 4	1	1	1
1:4	ORANGE 4 DUP	1	1	1
1:5	ORANGE 6	1	1	1
1:6	ORANGE 6 DUP	1	1	1
1:7	ORANGE 8	1	1	1
1:8	ORANGE 8 DUP	1	1	1
1:9	ORANGE 10	1	1	1
1:10	ORANGE 10 DUP	1	1	1
1:11	ORANGE 12	1	1	1
1:12	ORANGE 12 DUP	1	1	1
S1:7	RINSE	1	1	1
S1:11	Low QC Dup	1	1	1
S1:12	High QC Dup	1	1	1
1:13	BANANA 2	1	1	1
1:14	BANANA 2 DUP	1	1	1

b

Test Report

Rack:Tube	Sample Label	Weight (g)	Volume (mL)	Dilution
1:15	BANANA 4	1	1	1
1:16	BANANA 4 DUP	1	1	1
1:17	BANANA 6	1	1	1
1:18	BANANA 6 DUP	1	1	1
1:19	BANANA 8	1	1	1
1:20	BANANA 8 DUP	1	1	1
1:21	BANANA 10	1	1	1
1:22	BANANA 10 DUP	1	1	1
1:23	BANANA 12	1	1	1
1:24	BANANA 12 DUP	1	1	1
S1:7	RINSE	1	1	1
S1:1	Blank	1	1	1
S1:2	Standard 1	1	1	1
S1:3	Standard 2	1	1	1
S1:4	Standard 3	1	1	1
S1:5	Standard 4	1	1	1
S1:6	Standard 5	1	1	1
S1:11	Low QC Dup	1	1	1
S1:12	High QC Dup	1	1	1
1:25	CORN 2	1	1	1
1:26	CORN 2 DUP	1	1	1
1:27	CORN 4	1	1	1
1:28	CORN 4 DUP	1	1	1
1:29	CORN 6	1	1	1
1:30	CORN 6 DUP	1	1	1
1:31	CORN 8	1	1	1
1:32	CORN 8 DUP	1	1	1
1:33	CORN 10	1	1	1
1:34	CORN 10 DUP	1	1	1
1:35	CORN 12	1	1	1
1:36	CORN 12 DUP	1	1	1
S1:7	RINSE	1	1	1
S1:11	Low QC Dup	1	1	1
S1:12	High QC Dup	1	1	1
1:37	CONTROL 2	1	1	1
1:38	CONTROL 2 DUP	1	1	1
1:39	CONTROL 4	1	1	1
1:40	CONTROL 4 DUP	1	1	1
1:41	CONTROL 6	1	1	1
1:42	CONTROL 6 DUP	1	1	1
1:43	CONTROL 8	1	1	1
1:44	CONTROL 8 DUP	1	1	1
1:45	CONTROL 10	1	1	1
1:46	CONTROL 10 DUP	1	1	1
1:47	CONTROL 12	1	1	1
1:48	CONTROL 12 DUP	1	1	1
S1:7	RINSE	1	1	1
S1:11	Low QC Dup	1	1	1
S1:12	High QC Dup	1	1	1

Common Conditions

Replicate Count	3	Intelligent Rinse Enabled	False
Pump Speed (rpm)	12	AVS67 Enabled	False
Sample Uptake Time (s)	12	Uptake Delay (s)	
Sample Uptake Fast Pump	True	Uptake Rate (mL/min)	
Rinse Time (s)	30	Injection Rate (mL/min)	
Rinse Time Fast Pump	True	Bubble Injection Time (s)	
Rinse Port Position		Preemptive Rinse Time (s)	

Condition Set Title	**Condition Set: 1**
Read Time (s)	5
RF Power (KW)	1.2
Stabilization Time (s)	10
Viewing Mode	Radial
Viewing Height (mm)	8
Nebulizer Flow (L/min)	0.7
Plasma Flow (L/min)	12
Aux Flow (L/min)	1
Makeup Flow (L/min)	0
Oxygen Percent (%)	0

Calibrations

Standard Concentrations By Element

Solution Label	Se (ppm)
Blank	0.00
Standard 1	1.00
Standard 2	20.00
Standard 3	50.00
Standard 4	100.00
Standard 5	120.00

d

Test Report

Agilent Technologies

Summary Calibration Results

Element and wavelength	Type	Units	Correlation Coefficient	%RSE
Se (196.026 nm)	Analyte	ppm	0.99973	3.434498 12
Se (203.985 nm)	Analyte	ppm	0.99976	4.534546 49
Se (196.026 nm)	Analyte	ppm	0.99982	3.573055 60
Se (203.985 nm)	Analyte	ppm	0.99980	2.905096 37

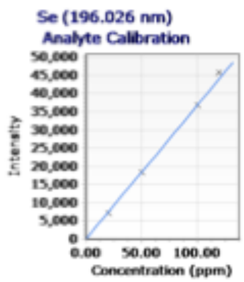

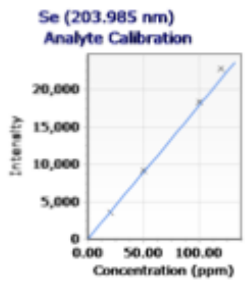

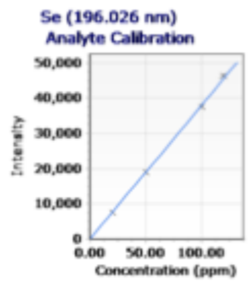

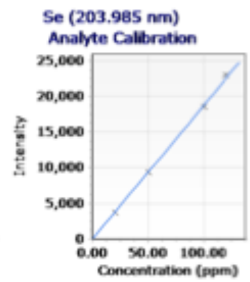

Results

Solution Label	Se (196.026 nm)	Se (203.985 nm)
Blank	0.00 (ppm)	0.00 (ppm)
Standard 1	1.00 e (ppm)	1.00 e (ppm)
Standard 2	20.00 e (ppm)	20.00 e (ppm)
Standard 3	50.00 e (ppm)	50.00 e (ppm)
Standard 4	100.00 e (ppm)	100.00 e (ppm)
Standard 5	120.00 e (ppm)	120.00 e (ppm)
Low QC Dup	9.82 (ppm)	9.92 (ppm)
High QC Dup	77.82 (ppm)	78.86 (ppm)
ORANGE 2	42.62 (ppm)	43.22 (ppm)
ORANGE 2 DUP	42.87 (ppm)	43.37 (ppm)
ORANGE 4	47.69 (ppm)	48.25 (ppm)
ORANGE 4 DUP	48.03 (ppm)	48.71 (ppm)
ORANGE 6	47.10 (ppm)	47.62 (ppm)
ORANGE 6 DUP	46.96 (ppm)	47.63 (ppm)

e

Solution Label	Se (196.026 nm)	Se (203.985 nm)
ORANGE 8	47.69 (ppm)	48.21 (ppm)
ORANGE 8 DUP	47.96 (ppm)	48.55 (ppm)
ORANGE 10	48.74 (ppm)	49.26 (ppm)
ORANGE 10 DUP	48.57 (ppm)	49.04 (ppm)
ORANGE 12	45.53 (ppm)	45.94 (ppm)
ORANGE 12 DUP	44.46 (ppm)	44.91 (ppm)
RINSE	0.04 (ppm)	0.06 (ppm)
Low QC Dup	10.03 (ppm)	10.17 (ppm)
High QC Dup	81.89 (ppm)	82.98 (ppm)
BANANA 2	46.53 (ppm)	46.88 (ppm)
BANANA 2 DUP	46.79 (ppm)	47.07 (ppm)
BANANA 4	48.28 (ppm)	48.99 (ppm)
BANANA 4 DUP	48.32 (ppm)	48.95 (ppm)
BANANA 6	46.42 (ppm)	46.88 (ppm)
BANANA 6 DUP	45.88 (ppm)	46.42 (ppm)
BANANA 8	47.72 (ppm)	48.19 (ppm)
BANANA 8 DUP	47.52 (ppm)	47.96 (ppm)
BANANA 10	48.38 (ppm)	48.84 (ppm)
BANANA 10 DUP	48.62 (ppm)	49.09 (ppm)
BANANA 12	47.38 (ppm)	47.92 (ppm)
BANANA 12 DUP	48.03 (ppm)	48.56 (ppm)
RINSE	0.07 (ppm)	0.04 u (ppm)
Blank	0.00 (ppm)	0.00 (ppm)
Standard 1	1.00 (ppm)	1.00 (ppm)
Standard 2	20.00 (ppm)	20.00 (ppm)
Standard 3	50.00 (ppm)	50.00 (ppm)
Standard 4	100.00 (ppm)	100.00 (ppm)
Standard 5	120.00 (ppm)	120.00 (ppm)
Low QC Dup	9.95 (ppm)	9.93 (ppm)
High QC Dup	80.38 (ppm)	80.19 (ppm)
CORN 2	46.46 (ppm)	46.39 (ppm)
CORN 2 DUP	46.72 (ppm)	46.56 (ppm)
CORN 4	48.99 (ppm)	48.68 (ppm)
CORN 4 DUP	49.52 (ppm)	49.46 (ppm)
CORN 6	47.38 (ppm)	47.15 (ppm)

f

Solution Label	Se (196.026 nm)	Se (203.985 nm)
CORN 6 DUP	47.62 (ppm)	47.50 (ppm)
CORN 8	48.37 (ppm)	48.22 (ppm)
CORN 8 DUP	48.19 (ppm)	47.98 (ppm)
CORN 10	37.94 (ppm)	37.71 (ppm)
CORN 10 DUP	38.09 (ppm)	38.00 (ppm)
CORN 12	47.67 (ppm)	47.48 (ppm)
CORN 12 DUP	47.61 (ppm)	47.36 (ppm)
RINSE	0.05 (ppm)	0.03 (ppm)
Low QC Dup	9.91 (ppm)	9.83 (ppm)
High QC Dup	80.84 (ppm)	80.62 (ppm)
CONTROL 2	44.65 (ppm)	44.47 (ppm)
CONTROL 2 DUP	44.94 (ppm)	44.86 (ppm)
CONTROL 4	49.88 (ppm)	49.74 (ppm)
CONTROL 4 DUP	50.05 (ppm)	49.93 (ppm)
CONTROL 6	48.69 (ppm)	48.39 (ppm)
CONTROL 6 DUP	49.14 (ppm)	48.82 (ppm)
CONTROL 8	50.31 (ppm)	50.05 (ppm)
CONTROL 8 DUP	50.25 (ppm)	50.03 (ppm)
CONTROL 10	51.45 (ppm)	51.10 (ppm)
CONTROL 10 DUP	51.24 (ppm)	51.08 (ppm)
CONTROL 12	45.25 (ppm)	45.00 (ppm)
CONTROL 12 DUP	45.06 (ppm)	44.80 (ppm)
RINSE	0.03 (ppm)	0.02 (ppm)
Low QC Dup	9.96 (ppm)	9.85 (ppm)
High QC Dup	81.33 (ppm)	80.76 (ppm)

A.2 Batch Adsorption Test ICP Data

Summary

Worksheet Name	GM Capstone Corn Batch Test.esws	Created Date/Time (local)	2025-03-31 2:42:08 PM
Instrument Name	MY2240CQ23	Created Date/Time (GMT)	2025-03-31 8:42:08 PM
Software Version	7.6.0.12121	Workstation Name	DESKTOP-7NFNNVR
Firmware Version	5590	Report Generated By	DESKTOP-7NFNNVR\ICP-OES

File Path D:\ICP-OES\Documents\Students\Worksheets\GM Capstone Corn Batch Test.esws

Notes

Elements

Element	Wavelength (nm)	Label	Type	Internal Standard	Background Correction	Calibration Fit	Condition Set
Se	196.026	Se (196.026 nm)	Analyte		Fitted	Linear Weighted	1
Se	203.985	Se (203.985 nm)	Analyte		Fitted	Linear Weighted	1

Sequence

Rack:Tube	Sample Label	Weight (g)	Volume (mL)	Dilution
S1:1	Blank	1	1	1
S1:2	Standard 1	1	1	1
S1:3	Standard 2	1	1	1
S1:4	Standard 3	1	1	1
S1:5	Standard 4	1	1	1
S1:6	Standard 5	1	1	1
S1:11	Low QC Dup	1	1	1
S1:12	High QC Dup	1	1	1
1:1	C:30 min 2 ppm	1	1	1
1:2	C:30 min 2 ppm dup	1	1	1
1:3	C:30 min 10 ppm	1	1	1
1:4	C:30 min 10 ppm dup	1	1	1
1:5	C:30 min 20 ppm	1	1	1
1:6	C:30 min 20 ppm dup	1	1	1
1:7	C:30 min 50 ppm	1	1	1
1:8	C:30 min 50 ppm dup	1	1	1
1:9	C:30 min 80 ppm	1	1	1
1:10	C:30 min 80 ppm dup	1	1	1
1:11	C:30 min 100 ppm	1	1	1
1:12	C:30 min 100 ppm dup	1	1	1
S1:7	RINSE	1	1	1
S1:11	Low QC Dup	1	1	1
S1:12	High QC Dup	1	1	1
1:13	C:60 min 2 ppm	1	1	1

Test Report

Agilent Technologies

Rack:Tube	Sample Label	Weight (g)	Volume (mL)	Dilution
1:14	C:60 min 2 ppm dup	1	1	1
1:15	C:60 min 10 ppm	1	1	1
1:16	C:60 min 10 ppm dup	1	1	1
1:17	C:60 min 20 ppm	1	1	1
1:18	C:60 min 20 ppm dup	1	1	1
1:19	C:60 min 50 ppm	1	1	1
1:20	C:60 min 50 ppm dup	1	1	1
1:21	C:60 min 80 ppm	1	1	1
1:22	C:60 min 80 ppm dup	1	1	1
1:23	C:60 min 100 ppm	1	1	1
1:24	C:60 min 100 ppm dup	1	1	1
S1:7	RINSE	1	1	1
S1:1	Blank	1	1	1
S1:2	Standard 1	1	1	1
S1:3	Standard 2	1	1	1
S1:4	Standard 3	1	1	1
S1:5	Standard 4	1	1	1
S1:6	Standard 5	1	1	1
S1:11	Low QC Dup	1	1	1
S1:12	High QC Dup	1	1	1
1:25	C:90 min 2 ppm	1	1	1
1:26	C:90 min 2 ppm dup	1	1	1
1:27	C:90 min 10 ppm	1	1	1
1:28	C:90 min 10 ppm dup	1	1	1
1:29	C:90 min 20 ppm	1	1	1
1:30	C:90 min 20 ppm dup	1	1	1
1:31	C:90 min 50 ppm	1	1	1
1:32	C:90 min 50 ppm dup	1	1	1
1:33	C:90 min 80 ppm	1	1	1
1:34	C:90 min 80 ppm dup	1	1	1
1:35	C:90 min 100 ppm	1	1	1
1:36	C:90 min 100 ppm dup	1	1	1
S1:7	RINSE	1	1	1
S1:11	Low QC Dup	1	1	1
S1:12	High QC Dup	1	1	1
1:37	C:120 min 2 ppm	1	1	1
1:38	C:120 min 2 ppm dup	1	1	1
1:39	C:120 min 10 ppm	1	1	1
1:40	C:120 min 10 ppm dup	1	1	1
1:41	C:120 min 20 ppm	1	1	1
1:42	C:120 min 20 ppm dup	1	1	1
1:43	C:120 min 50 ppm	1	1	1
1:44	C:120 min 50 ppm dup	1	1	1
1:45	C:120 min 80 ppm	1	1	1
1:46	C:120 min 80 ppm dup	1	1	1
1:47	C:120 min 100 ppm	1	1	1
1:48	C:120 min 100 ppm dup	1	1	1
S1:7	RINSE	1	1	1
S1:1	Blank	1	1	1

Test Report

Agilent Technologies

Rack:Tube	Sample Label	Weight (g)	Volume (mL)	Dilution
S1:2	Standard 1	1	1	1
S1:3	Standard 2	1	1	1
S1:4	Standard 3	1	1	1
S1:5	Standard 4	1	1	1
S1:6	Standard 5	1	1	1
S1:11	Low QC Dup	1	1	1
S1:12	High QC Dup	1	1	1
1:49	C:150 min 2 ppm	1	1	1
1:50	C:150 min 2 ppm dup	1	1	1
1:51	C:150 min 10 ppm	1	1	1
1:52	C:150 min 10 ppm dup	1	1	1
1:53	C:150 min 20 ppm	1	1	1
1:54	C:150 min 20 ppm dup	1	1	1
1:55	C:150 min 50 ppm	1	1	1
1:56	C:150 min 50 ppm dup	1	1	1
1:57	C:150 min 80 ppm	1	1	1
1:58	C:150 min 80 ppm dup	1	1	1
1:59	C:150 min 100 ppm	1	1	1
1:60	C:150 min 100 ppm dup	1	1	1
S1:7	RINSE	1	1	1
S1:11	Low QC Dup	1	1	1
S1:12	High QC Dup	1	1	1

Common Conditions

Replicate Count	4	Intelligent Rinse Enabled	False
Pump Speed (rpm)	12	AVS67 Enabled	False
Sample Uptake Time (s)	25	Uptake Delay (s)	
Sample Uptake Fast Pump	True	Uptake Rate (mL/min)	
Rinse Time (s)	30	Injection Rate (mL/min)	
Rinse Time Fast Pump	True	Bubble Injection Time (s)	
Rinse Port Position		Preemptive Rinse Time (s)	

k

Test Report

Agilent Technologies

Condition Set Title	**Condition Set: 1**
Read Time (s)	7
RF Power (KW)	1.2
Stabilization Time (s)	10
Viewing Mode	Radial
Viewing Height (mm)	8
Nebulizer Flow (L/min)	0.7
Plasma Flow (L/min)	12
Aux Flow (L/min)	1
Makeup Flow (L/min)	0
Oxygen Percent (%)	0

Calibrations

Standard Concentrations By Element

Solution Label	Se (ppm)
Blank	0.00
Standard 1	1.00
Standard 2	20.00
Standard 3	50.00
Standard 4	100.00
Standard 5	120.00

Summary Calibration Results

Element and wavelength	Type	Units	Correlation Coefficient	%RSE
Se (196.026 nm)	Analyte	ppm	0.99969	4.18003690
Se (203.985 nm)	Analyte	ppm	0.99967	2.00478050
Se (196.026 nm)	Analyte	ppm	0.99976	4.41208575

Test Report

Agilent Technologies

Element and wavelength	Type	Units	Correlation Coefficient	%RSE
Se (203.985 nm)	Analyte	ppm	0.99974	3.370284 13
Se (196.026 nm)	Analyte	ppm	0.99971	4.936866 17
Se (203.985 nm)	Analyte	ppm	0.99967	5.520008 22

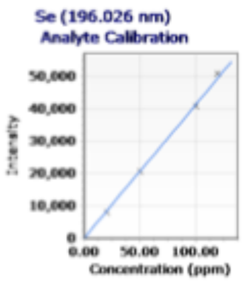

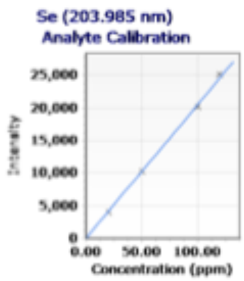

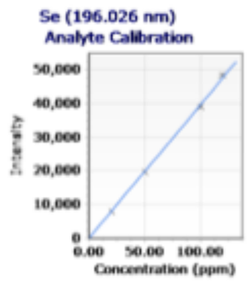

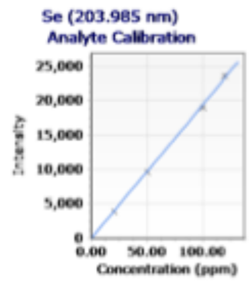

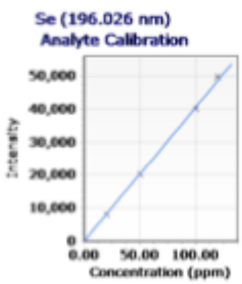

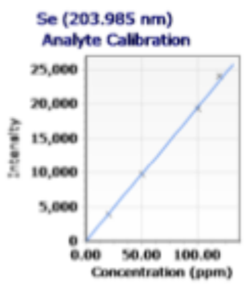

Results

Solution Label	Se (196.026 nm)	Se (203.985 nm)
Blank	0.00 (ppm)	0.00 (ppm)
Standard 1	1.00 (ppm)	1.00 (ppm)
Standard 2	20.00 (ppm)	20.00 (ppm)
Standard 3	50.00 (ppm)	50.00 (ppm)
Standard 4	100.00 (ppm)	100.00 (ppm)
Standard 5	120.00 (ppm)	120.00 (ppm)
Low QC Dup	9.89 (ppm)	9.84 (ppm)
High QC Dup	79.65 (ppm)	78.77 (ppm)
C:30 min 2 ppm	1.95 (ppm)	1.99 (ppm)

m

Test Report

Agilent Technologies

Solution Label	Se (196.026 nm)	Se (203.985 nm)
C:30 min 2 ppm dup	1.88 (ppm)	1.91 (ppm)
C:30 min 10 ppm	10.19 (ppm)	10.12 (ppm)
C:30 min 10 ppm dup	9.83 (ppm)	9.70 (ppm)
C:30 min 20 ppm	19.41 (ppm)	19.17 (ppm)
C:30 min 20 ppm dup	19.61 (ppm)	19.33 (ppm)
C:30 min 50 ppm	50.80 (ppm)	49.92 (ppm)
C:30 min 50 ppm dup	49.44 (ppm)	48.57 (ppm)
C:30 min 80 ppm	79.40 (ppm)	78.27 (ppm)
C:30 min 80 ppm dup	79.99 (ppm)	78.83 (ppm)
C:30 min 100 ppm	98.76 (ppm)	97.70 (ppm)
C:30 min 100 ppm dup	100.33 (ppm)	99.10 (ppm)
RINSE	0.05 (ppm)	0.11 (ppm)
Low QC Dup	10.03 (ppm)	9.90 (ppm)
High QC Dup	80.77 (ppm)	79.61 (ppm)
C:60 min 2 ppm	1.93 (ppm)	1.93 (ppm)
C:60 min 2 ppm dup	1.86 (ppm)	1.89 (ppm)
C:60 min 10 ppm	9.69 (ppm)	9.59 (ppm)
C:60 min 10 ppm dup	9.81 (ppm)	9.67 (ppm)
C:60 min 20 ppm	20.10 (ppm)	19.76 (ppm)
C:60 min 20 ppm dup	20.02 (ppm)	19.70 (ppm)
C:60 min 50 ppm	51.29 (ppm)	50.48 (ppm)
C:60 min 50 ppm dup	50.75 (ppm)	50.03 (ppm)
C:60 min 80 ppm	81.56 (ppm)	80.42 (ppm)
C:60 min 80 ppm dup	81.75 (ppm)	80.78 (ppm)
C:60 min 100 ppm	102.72 (ppm)	101.61 (ppm)
C:60 min 100 ppm dup	99.96 (ppm)	98.95 (ppm)
RINSE	0.05 (ppm)	0.11 (ppm)
Blank	0.00 ! (ppm)	0.00 ! (ppm)
Standard 1	1.00 ! (ppm)	1.00 ! (ppm)
Standard 2	20.00 ! (ppm)	20.00 ! (ppm)
Standard 3	50.00 ! (ppm)	50.00 ! (ppm)

n

Solution Label	Se (196.026 nm)	Se (203.985 nm)
Standard 4	100.00 ! (ppm)	100.00 ! (ppm)
Standard 5	120.00 ! (ppm)	120.00 ! (ppm)
Low QC Dup	9.76 ! (ppm)	9.66 ! (ppm)
High QC Dup	78.63 ! (ppm)	77.60 ! (ppm)
C:90 min 2 ppm	1.89 (ppm)	1.87 (ppm)
C:90 min 2 ppm dup	1.95 (ppm)	1.92 (ppm)
C:90 min 10 ppm	9.95 (ppm)	9.73 (ppm)
C:90 min 10 ppm dup	10.14 (ppm)	9.94 (ppm)
C:90 min 20 ppm	20.73 (ppm)	20.42 (ppm)
C:90 min 20 ppm dup	20.51 (ppm)	20.15 (ppm)
C:90 min 50 ppm	50.22 (ppm)	49.36 (ppm)
C:90 min 50 ppm dup	52.15 (ppm)	51.28 (ppm)
C:90 min 80 ppm	79.57 (ppm)	78.24 (ppm)
C:90 min 80 ppm dup	83.28 (ppm)	81.80 (ppm)
C:90 min 100 ppm	103.47 (ppm)	102.31 (ppm)
C:90 min 100 ppm dup	98.93 (ppm)	97.71 (ppm)
Low QC Dup	9.91 (ppm)	9.77 (ppm)
High QC Dup	80.17 (ppm)	78.64 (ppm)
C:120 min 2 ppm	1.96 (ppm)	1.91 (ppm)
C:120 min 2 ppm dup	1.81 (ppm)	1.78 (ppm)
C:120 min 10 ppm	9.97 (ppm)	9.81 (ppm)
C:120 min 10 ppm dup	9.70 (ppm)	9.51 (ppm)
C:120 min 20 ppm	20.49 (ppm)	20.11 (ppm)
C:120 min 20 ppm dup	20.49 (ppm)	20.09 (ppm)
C:120 min 50 ppm	51.70 (ppm)	50.69 (ppm)
C:120 min 50 ppm dup	51.18 (ppm)	50.28 (ppm)
C:120 min 80 ppm	80.61 (ppm)	79.33 (ppm)
C:120 min 80 ppm dup	84.27 (ppm)	82.80 (ppm)
C:120 min 100 ppm	101.89 (ppm)	100.50 (ppm)
C:120 min 100 ppm dup	102.81 (ppm)	101.59 (ppm)
Blank	0.00 (ppm)	0.00 (ppm)

Solution Label	Se (196.026 nm)	Se (203.985 nm)
Standard 1	1.00 (ppm)	1.00 (ppm)
Standard 2	20.00 (ppm)	20.00 (ppm)
Standard 3	50.00 (ppm)	50.00 (ppm)
Standard 4	100.00 (ppm)	100.00 (ppm)
Standard 5	120.00 (ppm)	120.00 (ppm)
Low QC Dup	9.76 (ppm)	9.74 (ppm)
High QC Dup	79.26 (ppm)	79.06 (ppm)
C:150 min 2 ppm	1.83 (ppm)	1.85 (ppm)
C:150 min 2 ppm dup	1.76 (ppm)	1.76 (ppm)
C:150 min 10 ppm	9.82 (ppm)	9.80 (ppm)
C:150 min 10 ppm dup	9.70 (ppm)	9.66 (ppm)
C:150 min 20 ppm	19.73 (ppm)	19.69 (ppm)
C:150 min 20 ppm dup	19.57 (ppm)	19.48 (ppm)
C:150 min 50 ppm	51.21 (ppm)	50.83 (ppm)
C:150 min 50 ppm dup	51.01 (ppm)	50.78 (ppm)
C:150 min 80 ppm	80.32 (ppm)	80.03 (ppm)
C:150 min 80 ppm dup	83.26 (ppm)	82.98 (ppm)
C:150 min 100 ppm	99.64 (ppm)	99.82 (ppm)
C:150 min 100 ppm dup	101.25 (ppm)	101.25 (ppm)
Low QC Dup	9.97 (ppm)	9.91 (ppm)
High QC Dup	80.14 (ppm)	79.69 (ppm)

p